Chromyl Chloride Chemistry on the TiO_2(110) Surface

M. Alam*

Department of Materials Engineering, New Mexico Institute of Mining and Technology, Socorro, New Mexico 87801

M. A. Henderson,* P. D. Kaviratna, G. S. Herman, and C. H. F. Peden

Environmental Molecular Sciences Laboratory, Pacific Northwest National Laboratory,† Richland, Washington 99352

Received: April 24, 1997; In Final Form: August 30, 1997⊗

The surface chemistry of chromyl chloride (CrO_2Cl_2) on TiO_2(110) was examined with TPD, AES, $\Delta\Phi$ measurements, SSIMS, and XPS. CrO_2Cl_2 adsorbs on TiO_2(110) at 130 K with a constant, coverage-independent sticking probability, which is presumably near unity based on TPD. $\Delta\Phi$ data suggest the molecule is adsorbed with the oxygens bound to the surface and the chlorines pointing into vacuum. In TPD, multilayer CrO_2Cl_2 desorption occurs at 156 K, and monolayer desorption states occur at about 295 and 430 K. Approximately 0.09 ML (1 ML = 5.2×10^{14} sites/cm^2) desorbs in each of the latter states. The remaining adsorbed CrO_2Cl_2 (0.48 ML) decomposes irreversibly above 500 K, eventually resulting in $CrCl_2$ desorption above 700 K. No other decomposition products are observed in TPD. Adsorption of CrO_2Cl_2 at 585 K results in multilayer $CrCl_2$ formation, while adsorption at or below 500 K results in a saturated monolayer. Between 500 and 700 K, XPS results suggest that the Cr deposited from CrO_2Cl_2 decomposition is reduced, possibly as the result of charge transfer from the defects in the n-doped TiO_2(110). SSIMS experiments conducted on the ^{18}O-enriched TiO_2(110) indicate that ^{16}O brought in by CrO_2Cl_2 is incorporated into the surface, whereas TPD indicates that only a small fraction of this incorporated ^{16}O is due to isotopic exchange into the desorbing parent at 400 K. Since no oxygen-containing decomposition products were observed in TPD, the decomposition of CrO_2Cl_2 on TiO_2(110) involves reaction at reduced surface sites (oxygen vacancies). As evidence for this, SSIMS indicates that the reaction of $^{18}O_2$ with $Ti^{16}O_2$(110) resulting in ^{18}O incorporation proceeds above 520 K presumably by the formation of oxygen vacancies from $^{16}O_2$ desorption. These results suggest that the reduction and potential immobilization of Cr(VI) species on TiO_2 materials may occur thermally if the appropriate surface defect sites are present.

1. Introduction

Chromium and its compounds are widely used in the industry.[1] The users of these materials eventually produce chromium-containing aqueous waste solutions in which chromium is present either in the trivalent state, Cr(III), or in the hexavalent state, Cr(VI).[1] In the trivalent state, chromium is present as a hydrated Cr^{3+} cation, while in the hexavalent state, it is present as a component of anions such as hydrated $Cr_2O_7^{2-}$, $HCrO_4^-$ or CrO_4^{2-}. Trivalent chromium is not hazardous, but hexavalent chromium is both toxic and carcinogenic.[2] The perilous nature of hexavalent chromium has prompted the regulatory agencies to classify Cr(VI)-bearing aqueous wastes as hazardous and to restrict their disposal directly onto or into the soil.[3] These restrictions have generated interest in developing new technologies for converting Cr(VI) to Cr(III). One such technology of interest involves photoreduction at the surface of compound semiconductor particles such as TiO_2.[4−9] Reduction of Cr(VI)−oxyanions by the photogenerated electrons is feasible only if the oxyanions are adsorbed onto the TiO_2 surface prior to photon irradiation. This is a necessary condition because transport of oxyanions from the bulk solution to the TiO_2 surface (where the photogenerated electrons are available) is slower than the electron−hole recombination process. Owing to the heterogeneous nature of the reaction, the interactions of Cr(VI)−oxyanions with TiO_2 surfaces play critical roles in the overall process. Despite their importance, such interactions have remained largely unexplored. Current understanding of these interactions is based exclusively on studies dealing with the adsorption behavior of CrO_4^{2-} anions at water−iron oxide interfaces[10,11] and of Cr^{3+} cations at water−alumina interfaces.[12] These studies, however, deal strictly with the adsorption kinetics where the data have been interpreted in terms of surface complexation models. The global objective of this study is to understand the thermal chemistry of Cr(VI)-bearing molecules adsorbed onto a well-characterized TiO_2 surface in the absence (this work) and presence of coadsorbed water.[13] Knowledge of the thermal processes will help future efforts guided to understanding the photoprocesses.

The Cr(VI)-bearing molecule chosen for this study was chromyl chloride (CrO_2Cl_2) in which chromium is in a tetrahedral environment. At room temperature, it is a liquid having a vapor pressure of about 10 Torr.[14] Although CrO_2Cl_2 is not important in and of itself, it was chosen because of the ease of introduction into the ultrahigh vacuum (UHV), contains chromium in the hexavalent state, and can undergo hydrolysis on contact with water yielding H_2CrO_4 or its dissociation

* To whom correspondence should be addressed.

† Pacific Northwest National Laboratory is a multiprogram national laboratory operated for the U.S. Department of Energy by Battelle Memorial Institute under Contract DE-AC06-76RLO 1830.

⊗ Abstract published in *Advance ACS Abstracts,* December 1, 1997.

S1089-5647(97)01386-2 CCC: $15.00
Published on Web 01/01/1998

products $HCrO_4^-$ and CrO_4^{2-}.[15] Thus, CrO_2Cl_2 adsorbed onto a surface in UHV has the potential to provide Cr(VI)−oxyanions upon reaction with codeposited water. The thermal induced chemistry and photochemistry of these Cr(VI)−oxyanionic species adsorbed on a surface in UHV can therefore be studied. Chromyl chloride was dosed onto clean TiO_2(110) surfaces in ultrahigh vacuum at low temperatures with and without codeposition of water. Surface chemistry was then studied using temperature-programmed desorption (TPD), Auger electron spectroscopy (AES), static secondary ion mass spectrometry (SSIMS), work function change measurement ($\Delta\Phi$), and X-ray photoelectron spectroscopy (XPS). To the authors' knowledge, no information regarding the interactions of Cr(VI)-containing inorganic molecules such as chromyl chloride with polycrystalline or single-crystal TiO_2 is available in the published literature, although there are published accounts dealing with chromyl chloride adsorption on other oxide materials.[16−19] This paper deals with the thermal induced chemistry of chromyl chloride at the TiO_2(110) surface in the absence of coadsorbed water. More specifically, the objectives of the study are to understand the binding of chromyl chloride with the TiO_2(110) surface, to quantify the partitioning between the desorbed and the decomposed chromyl chloride, and to determine the chromyl chloride decomposition pathways. Chromyl chloride chemistry at the TiO_2(110) surface in the presence of water will be discussed in a subsequent paper.[13]

2. Experimental Section

Two separate UHV chambers were used in this study. The first chamber, described in more detail elsewhere,[20] housed a quadrupole mass spectrometer (QMS) for temperature-programmed desorption (TPD) and +/− static secondary ion mass spectrometry (SSIMS) measurements, a double-pass cylindrical mirror analyzer (DPCMA) for Auger electron spectroscopy (AES) and work function change measurements, rear-view low-energy electron diffraction (LEED) optics, and a high-resolution electron energy loss spectrometer (HREELS). Temperature-programmed studies were performed using resistive heating of a Ta backing plate (see below) and a 2 K/s temperature ramp. All SSIMS measurements utilized a 500 V primary Ar^+ beam focused on the crystal to a spot approximately 2 mm in diameter. The primary ion beam flux for all SSIMS measurements was 10 nA/cm^2, ensuring that the maximum total primary ion exposure during any SSIMS experiment was maintained below 5% of a monolayer. By the word "monolayer" we mean the "first layer" as opposed to the letters "ML" which we will use to refer to the "number of sites per unit area". It should be noted that since TPD and temperature-programmed SSIMS measurements will be discussed throughout this paper, the reader should take care to differentiate between the QMS signals from these two techniques. This is especially important for Cr (m/e = 52) signals, which in TPD result from QMS cracking of the CrO_2Cl_2 and $CrCl_x$ desorption species, and in SSIMS from sputtering of Cr ions from species on the TiO_2(110) surface. For this reason, we will refer to TPD signals as neutral species (Cr) and SSIMS signals as ions, but the reader should notice that the former implies electron impact cracking of some parent species. Work function change measurements ($\Delta\Phi$) were obtained with the DPCMA using the onset of secondary electron emission from a 200 V primary electron beam and with a −20 V bias on the crystal. AES measurements were recorded using a lock-in amplifier and a 3 kV primary electron beam. Care was taken in both AES and $\Delta\Phi$ measurements to minimize exposure of the adlayer to the electron beam. For experiments in which coverage or temperature were varied, different spots on the crystal were sampled.

X-ray photoelectron spectroscopic (XPS) measurements were carried out in the second UHV chamber (without liquid nitrogen cooling). This chamber was equipped with a single-pass CMA for AES, LEED optics, and a Physical Electronics Model 5400 hemispherical analyzer equipped with a dual-anode (Al and Mg) nonmonochromatic X-ray source for XPS measurements. For the studies reported here, the Mg anode was operated at 12.5 kV and 300 W, and the electron energy analyzer was operated in the constant analyzer energy mode at a pass energy of 50 eV. These operating conditions gave a working instrument resolution (including broadening due to X-ray width), defined as the full width at half-maximum (fwhm), of 1.0 eV. All binding energies (BEs) are referenced to the Fermi level of gold [Au($4f_{7/2}$) = 84.0 eV] and were reproducible to ±0.02 eV. The curve fitting of XPS spectra were carried out using Rainbow software with a Gaussian/Lorentzian product function and an integrated Shirley background. Both chambers had base pressures of $<2 \times 10^{-10}$ Torr.

The same TiO_2(110) crystal was used in experiments in either chamber. The crystal was mounted on a polished Ta plate using a thin film of In, as described previously.[21] The only difference in the mounting of the crystal in the two chambers was that a type K (Cr−Al) thermocouple was used in the TPD/SSIMS chamber and a type C (W−Re) was used in the XPS chamber. Because of this, we observed an approximately 50 K difference (higher for the XPS chamber) between the temperatures at which identical processes (e.g., $CrCl_x$ desorption) occurred from TiO_2-(110) in these two chambers. This temperature difference was not deemed significant and thus was not compensated for in comparisons of data between the two chambers. After each CrO_2Cl_2 experiment the surface was sputtered with 3 kV Ar^+ until the $^{52}Cr^+$ SSIMS signal was less than 1% of the total Ti^+ signal. Removal of the Cr typically required a total 3 kV Ar^+ exposure of about 10 mC/cm^2 (about 120 ML of Ar^+), whereas the chlorine was removed by annealing at 820 K prior to sputtering. After 3 kV sputtering the surface was smoothed by sputtering with 500 V Ar^+, then oxidized in 1×10^{-7} Torr O_2 at 820 K for 10 min followed by cooling in O_2 to below 400 K. By use of $^{18}O_2$ instead of $^{16}O_2$, the surface could be converted to $Ti^{18}O_2$(110). The natural isotopic abundance of oxygen was restored easily by sputtering off the thin ^{18}O-containing layer.

One point regarding the TiO_2(110) crystal is of importance. As a result of extensive annealing in vacuum above 850 K (in a previous and unrelated study), this crystal reached a point in which the surface charge associated with the creation of oxygen vacancies by O_2 desorption during annealing could not be readily accommodated in the bulk of the oxide. Therefore, some of these vacancies persisted on the surface, presumably as isolated sites, even after cooling the oxidized surface to room temperature in O_2. The coverage of these sites was about $(2.5-5.0) \times 10^{13}$ per cm^2 based on water TPD.[22] Unfortunately, at the time we conducted these experiments we did not know that these isolated sites could be completely filled by maintaining a large oxygen flux on the crystal at room temperature for a period of 30 min.[23] As will be shown, the presence of these isolated defect sites had a minor but noticeable effect on the properties of CrO_2Cl_2 on TiO_2(110).

Chromyl chloride (ACS reagent grade, 99.99+% purity) was obtained from Aldrich in a darkened glass amulet and was transferred under dry N_2 atmosphere to a stainless steel vessel. It was then purified by several freeze−pump−thaw cycles using liquid nitrogen before use. This procedure successfully removed

TABLE 1: QMS Signals Monitored during TPD of Varying Exposures of CrO_2Cl_2 on Clean TiO_2(110) Surface at 130 K[a]

species	*m/e*	species	*m/e*	species	*m/e*
O (†)	16	Ti (†)	48	Cr (p)	52
O_2 (*)	32	TiO (*)	64	CrO (p)	68
Cl (*)	35	TiO_2 (*)	80	CrO_2 (p)	84
Cl_2 (*)	70	TiOCl (*)	99	CrCl (p)	87
OCl (p)	51	$TiOCl_2$ (*)	134	$CrCl_2$ (p)	124
OCl_2 (p)	86	TiCl (†)	83	$CrCl_3$ (*)	159
		$TiCl_2$ (†)	118	CrOCl (p)	103
		$TiCl_3$ (†)	153	CrO_2Cl (p)	119
		$TiCl_4$ (*)	190	$CrOCl_2$ (p)	138
				CrO_2Cl_2	154

[a] No signal (*), trace signal (†), parent CrO_2Cl_2 cracking fragment (p).

HCl and Cl_2 impurities that presumably resulted from the transfer and/or initial contact of CrO_2Cl_2 with the stainless steel vessel. The gas handling system was accommodated to CrO_2Cl_2 after a few 10 Torr exposures. After this treatment there was no sign of impurities in the dosed gas. To further ensure the purity of the dosed CrO_2Cl_2, the gas line was evacuated at the start of each day, and new CrO_2Cl_2 vapor was used. CrO_2Cl_2 was dosed on the crystal through a calibrated pinhole aperture doser described previously.[20] The best results were obtained upon retracting the crystal from the doser by 5 mm, maintaining a steady flow of gas through the doser (that corresponded to a flux of about 2.0×10^{13} molecules cm^{-2} s^{-1} at the crystal, when the doser was next to the crystal) and using a flag to start and stop each dose. The exposed area on the retracted crystal was approximately the same as when the crystal was against the doser based on comparisons of the TPD intensities from the two dosing methods.

3. Results and Discussion

3.1. Results from Adsorption at 130 K. No ordered LEED patterns and no new HREELS loss features were observed for chromyl chloride adsorbed on TiO_2(110). The absence of ordered LEED patterns for adsorbed CrO_2Cl_2 may result from sensitivity of this species to dissociative electron attachment processes initiated by the LEED beam. For the case of HREELS, all the vibrational modes of the parent molecule are located below 1000 cm^{-1} and were obscured by the intense primary phonon modes of TiO_2.

3.1.1. TPD Results. Preliminary experiments were carried out to identify the products of desorption of the parent molecule CrO_2Cl_2 (*m/e* = 154) that was adsorbed onto the clean TiO_2(110) surface at 130 K. The TPD spectra were obtained up to 820 K. A number of possible QMS signals were monitored. These are listed in Table 1. No O_x, Cl_x, TiO_x, $TiOCl_x$, and CrO_x (where *x* varied between 1 and 2) species desorbed from the surface. The $TiCl_x$ (*x* between 1 and 4) QMS cracking fragments registered identical spectra that were similar to that of Ti (*m/e* = 48). Similarly, the $CrCl_x$ (*x* between 1 and 3) fragments registered identical spectra that were similar to that of Cr (*m/e* = 52). For both types of species, the signal intensity decreased with increasing *x*. Also, $CrCl_x$ signals were strong while the $TiCl_x$ signals were very weak. The OCl_x and the CrO_xCl_y (*y* varying from 1 to 2) molecules exhibited similar spectra (except in intensity) that were identical with that of CrO_2Cl_2 and less intense than $CrCl_x$. TPD experiments indicated that the detectable desorption products were $CrCl_x$, the parent molecule CrO_2Cl_2, and $TiCl_x$.

TPD spectra were obtained up to 820 K after exposing clean TiO_2(110) at 130 K to different exposures of CrO_2Cl_2 varying between 0.3×10^{14} and 8.4×10^{14} molecules/cm^2. The desorption spectra for the Ti (*m/e* = 48), Cr (*m/e* = 52), CrCl (*m/e* = 87), CrOCl (*m/e* = 103), and CrO_2Cl_2 (*m/e* = 154) QMS signals obtained from CrO_2Cl_2 exposure of 3.7×10^{14} molecules/cm^2 are presented in Figure 1. It is apparent that Cr and CrCl spectra trace each other over the entire temperature range. This was also true for $CrCl_2$, although the signal from this species was weak (not shown). Similarly, CrOCl and CrO_2Cl_2 spectra are alike. The desorption products are, therefore, CrO_2Cl_2 desorbing at temperatures below 500 K, $CrCl_x$ desorbing above 710 K, and a Ti-bearing species desorbing at 793 K. In one case, the spectra were obtained up to 850 K and indicated the $CrCl_x$ peak to be at 835 K. The spectra of the five species at other exposures were identical except in intensity. Perusal of the figure indicates that the Cr (*m/e* = 52) QMS signal exhibits desorption peaks from both the Cr-bearing desorption products CrO_2Cl_2 and $CrCl_x$. Therefore, the *m/e* = 52 QMS signal was monitored to evaluate the coverage-dependent effects of both of these desorption products.

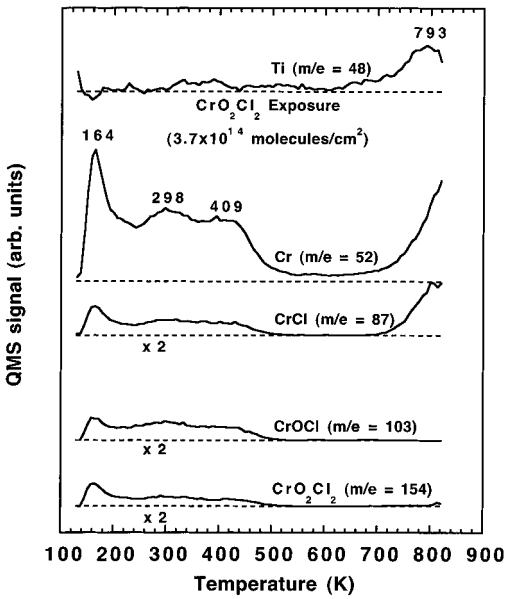

Figure 1. TPD spectra from a CrO_2Cl_2 exposure of 3.7×10^{14} molecules/cm^2 to the clean TiO_2(110) surface at 130 K. Spectra are displaced vertically for clarity and baselines are shown to highlight important TPD features.

The TPD spectra for the Cr (*m/e* = 52) QMS signal resulting from various exposures of CrO_2Cl_2 are presented in Figure 2. Up to exposures of 1.7×10^{14} molecules/cm^2, little or no desorption of CrO_2Cl_2 occurred (absence of low-temperature desorption peaks), indicating complete irreversible decomposition of the parent molecule and subsequent desorption of the $CrCl_x$ decomposition product at 730 K. At a CrO_2Cl_2 exposure of 2.5×10^{14} molecules/cm^2, a single CrO_2Cl_2 desorption state appears at 439 K. At a higher CrO_2Cl_2 exposure, another CrO_2Cl_2 desorption state appears at 305 K. As exposure increases, both of the desorption states grow in intensity and shift to lower temperatures. The low-temperature state (appearing initially at 305 K) saturates at 293 K, while the high-temperature state (appearing initially at 439 K) saturates at 429 K. As these desorption states saturate, another peak due to multilayer formation appears at 175 K. This peak could not be saturated with increasing exposure and continued to shift to about 156 K before becoming independent of exposure.

The low-temperature state between 293 and 305 K is attributed to desorption of CrO_2Cl_2 from the "crowded" monolayer because this state appears at high exposures (>2.5×10^{14}

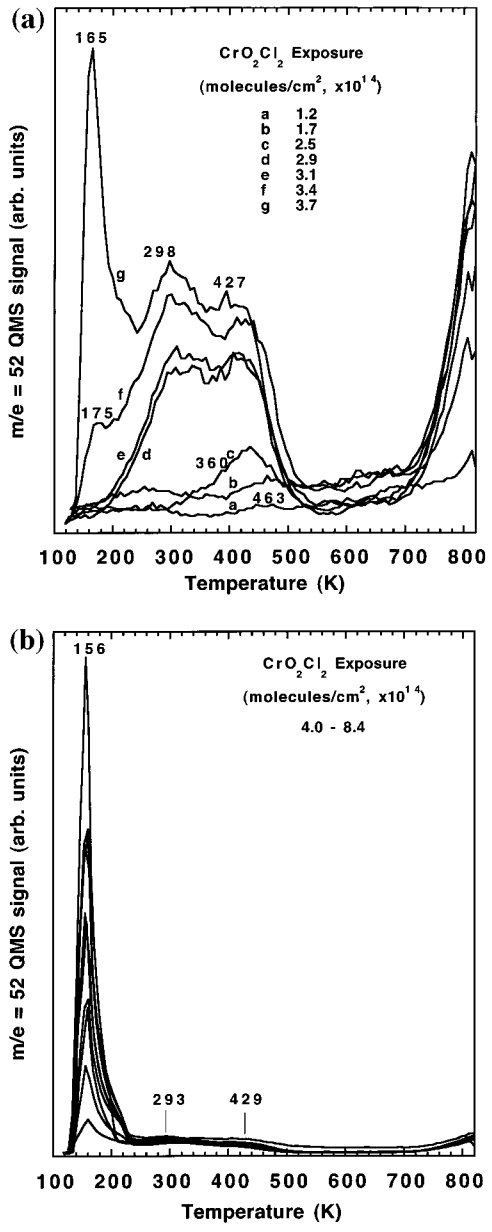

Figure 2. TPD spectra of the Cr^+ ($m/e = 52$) QMS cracking fragment as a function of CrO_2Cl_2 exposure to the clean TiO_2(110) surfaces at 130 K.

molecules/cm^2). The high-temperature state between 429 and 439 K is attributed to desorption of CrO_2Cl_2 from defect sites as discussed below. By use of a first-order Redhead's approximation[24] ($E = 0.06T_P$, where T_P is the saturated peak temperature), the heats of desorption of CrO_2Cl_2 from the low-temperature and the high-temperature states were estimated (within ±20%) to be 75 and 109 kJ/mol, respectively. The high-temperature state could also be a result of recombinative desorption of the decomposition products of CrO_2Cl_2 (to be discussed).

The area under the Cr ($m/e = 52$) desorption curves between 210 and 600 K (due to desorption of monolayer CrO_2Cl_2) versus the CrO_2Cl_2 exposure is plotted in Figure 3 (squares). The peak area is near zero at low exposures but increases with higher exposures and eventually becomes constant (within the range of experimental error) as saturation is reached. The figure indicates that complete monolayer coverage of the TiO_2(110) surface is obtained at a CrO_2Cl_2 exposure of about 3.4×10^{14} molecules/cm^2, which is roughly 65% of the total number of

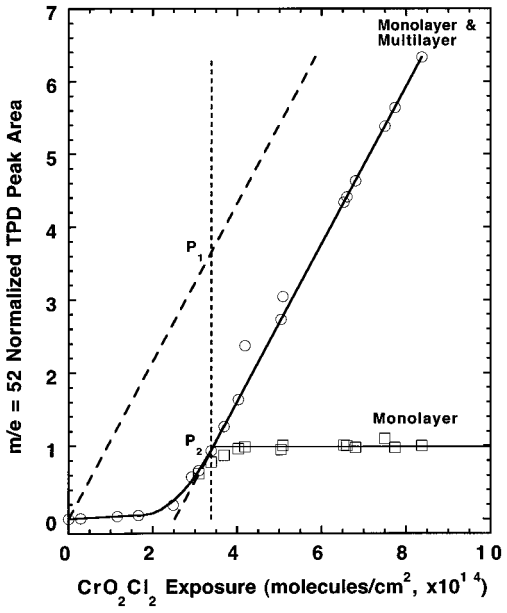

Figure 3. Normalized TPD peak areas under the monolayer (210−600 K, □) and multilayer + monolayer (130−600 K, ○) peaks for the Cr^+ ($m/e = 52$) QMS cracking fragment as a function of CrO_2Cl_2 exposure to clean TiO_2(110) surfaces at 130 K.

five-coordinate Ti^{4+} adsorption sites on the TiO_2(110) surface (5.2×10^{14} molecules/cm^2). This suggests that each adsorbed CrO_2Cl_2 molecule occupies/blocks about two Ti^{4+} surface sites, indicating that the adsorbed molecule is much larger in size than the site-to-site distance.

The total area under the Cr ($m/e = 52$) desorption curve up to 600 K (due to multilayer and monolayer desorption of CrO_2Cl_2) versus the CrO_2Cl_2 exposure is also shown in Figure 3 (circles). Two different domains can be identified. At low exposures (corresponding to submonolayer coverages), the data follow linear behavior with the line passing through the origin. At high exposures, the data form a straight line of much greater slope off-center from the origin. This uptake region corresponds to multilayer formation. Given the fact that the adsorption temperature is below the leading edge of the multilayer state (see Figure 2), we assume unity sticking coefficient for this constant uptake. The same unity sticking coefficient is also assumed for the monolayer states. These data indicate that in the low-exposure regime, most of the CrO_2Cl_2 irreversibly decomposes on the clean TiO_2(110) surface (i.e., it is not recovered in TPD). To determine the extent of dissociative versus molecular desorption, a line was drawn through the origin and parallel to the high-coverage linear portion of the plot (dashed). The ratio of the point on the solid line (P_2) with that on the dashed line (P_1) at monolayer saturation (3.4×10^{14} molecules/cm^2 or 0.65 ML) is representative of the degree of molecular desorption. The data indicate that 74% (2.5×10^{14} molecules/cm^2 or 0.48 ML) of the CrO_2Cl_2 monolayer irreversibly decomposes and only 26% (0.9×10^{14} molecules/cm^2 or 0.17 ML) desorbs as molecular CrO_2Cl_2.

3.1.2. AES Results. Auger electron spectroscopy (AES) was performed to quantify the Cl content of the TiO_2(110) surface. The clean TiO_2(110) surface did not exhibit a Cl signal (Figure 4a), but surfaces exposed to CrO_2Cl_2 exhibited a Cl signal at 180 eV. However, the dominant AES signal for Cr at 520 eV was not detected, either for monolayer quantities of CrO_2Cl_2 or after CrO_2Cl_2 decomposition. This absence of a Cr AES signal presumably is because it was lost in the tail of the strong O(KLL) signal at 504 eV. A weak Cr signal was observed after

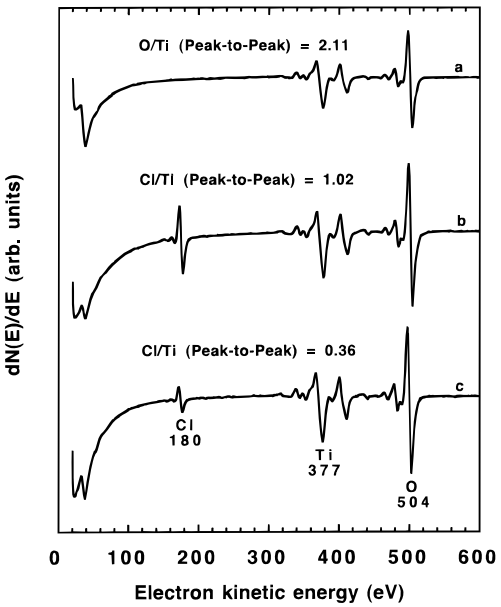

Figure 4. AES spectra of (a) the clean TiO_2(110) surface and of the TiO_2(110) surface after CrO_2Cl_2 exposure of 8.4×10^{14} molecules/cm^2 at 130 K followed by heating to (b) 600 K and (c) 800 K.

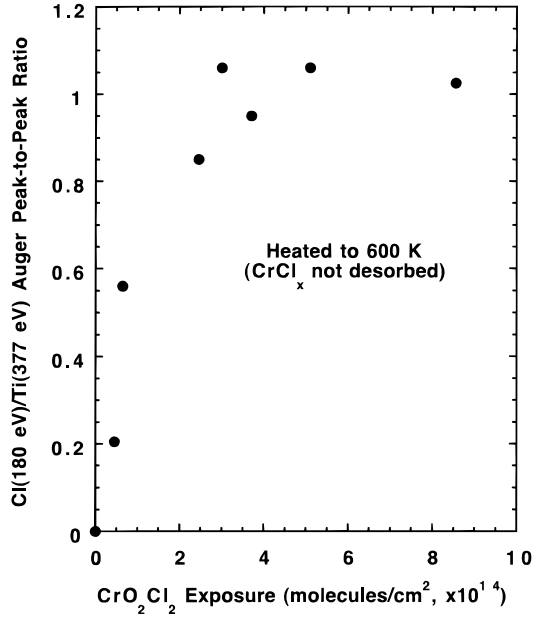

Figure 5. Cl (180 eV)/Ti (377 eV) Auger peak-to-peak ratio as a function of CrO_2Cl_2 exposure to clean TiO_2(110) surface at 130 K. Auger spectra taken after heating to 600 K.

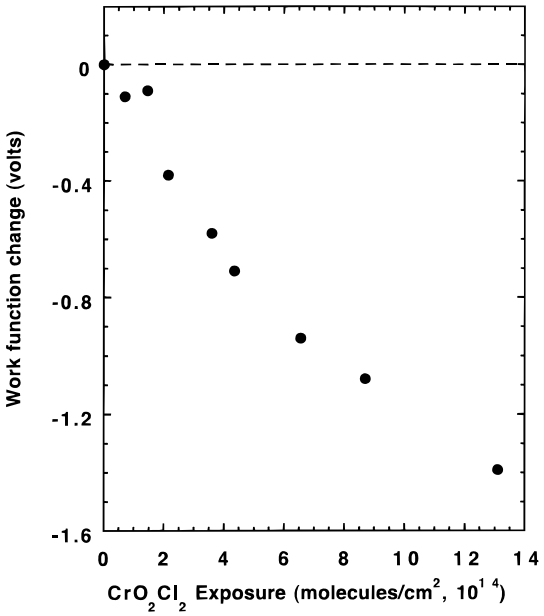

Figure 6. Work function change as a function of CrO_2Cl_2 exposure to the clean TiO_2(110) surface at 130 K.

dosing CrO_2Cl_2 at 585 K (see below), but this signal was still partially obscured by the O signal.

The AES of two TiO_2(110) surfaces that were exposed to CrO_2Cl_2 exposure of 8.4×10^{14} molecules/cm^2 at 130 K and subsequently heated to 600 and 820 K are presented in parts b and c of Figure 4, respectively. Clearly, the Cl surface coverage decreases as the upper limit of temperature during TPD increases from 600 to 820 K; however, not all the Cl has been removed at 820 K. This is in agreement with the TPD data (Figures 1 and 2), which indicate that $CrCl_x$ desorbs above 710 K but does not peak until 835 K. Assuming that all the Cl signal at 600 K is the result of 2.5×10^{14} molecules/cm^2 of CrO_2Cl_2 decomposition (see above), then roughly 1.8×10^{14} Cl atoms/cm^2 remain on the surface after heating to 820 K.

The peak-to-peak ratio of the Cl signal (at 180 eV) to that of the Ti signal (at 377 eV) was used as an indicator of the chlorine coverage left on the surface after TPD of CrO_2Cl_2 to 600 K (no $CrCl_x$ desorption). These data are shown in Figure 5. The figure indicates that initially, the surface chlorine content increases with increasing CrO_2Cl_2 exposure and then levels off at higher exposures. The leveling-off of the ratio occurs at about 4×10^{14} molecules/cm^2, which is approximately where the monolayer saturates based on TPD (Figure 3).

3.1.3. Work Function Change Results. Work function change, $\Delta\Phi$, measurements were carried out for CrO_2Cl_2 adsorbed on clean TiO_2 surfaces as a function of (a) CrO_2Cl_2 exposure at 130 K and (b) annealing temperature for CrO_2Cl_2 exposure of 8.5×10^{14} molecules/cm^2 adsorbed at 130 K. The effect of CrO_2Cl_2 exposure on $\Delta\Phi$ is presented in Figure 6. The work function decreases to more negative values as the exposure increases. Since SSIMS and XPS results (to be discussed) suggest that adsorbed CrO_2Cl_2 does not decompose on TiO_2(110) until the temperature has exceeded 500 K, we can construct a model for the structure of a saturated monolayer that draws from the $\Delta\Phi$ measurements and the TPD data discussed above. The negative work function change suggests that the adsorbed molecule is oriented with the positive end of the molecule away from the surface and the negative end toward the surface. Based on calculations by Pershina and Fricke,[25] the molecular dipole moment of CrO_2Cl_2 is 0.88 D with the negative end of the dipole between the oxygen atoms and the positive end between the chlorine atoms. This would place the adsorbed molecule on TiO_2(110) with the oxygen atoms pointing toward the surface and the chlorine atoms pointing toward vacuum. In the absence of a significant charge redistribution, this orientation of the molecule would favor a bidentate bonding geometry, presumably with the oxygen atoms bridging two five-coordinate Ti^{4+} cations, as in the case of formate on TiO_2(110).[26] Given that the Cl−Cl distance within a CrO_2Cl_2 molecule is about 3.55 Å [27] and that the TiO_2(110) unit cell is 2.96 Å by 6.49 Å (along the [001] and [1$\bar{1}$0] directions, respectively), the Cl−Cl distance between Cl atoms on two adjacent bidentate CrO_2Cl_2 molecules (with unperturbed gas-phase structures) should be about 5.92 Å along the [001] direction and 2.94 Å along the [1$\bar{1}$0] direction. The former distance is compatible with the 1.8 Å van der Waals' radius of Cl. However, the latter

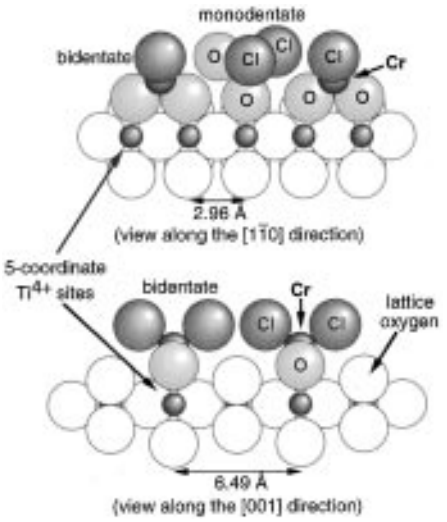

Figure 7. Hypothetical model for the structure of monolayer saturation CrO_2Cl_2 on TiO_2(110) based on work function change and TPD measurements.

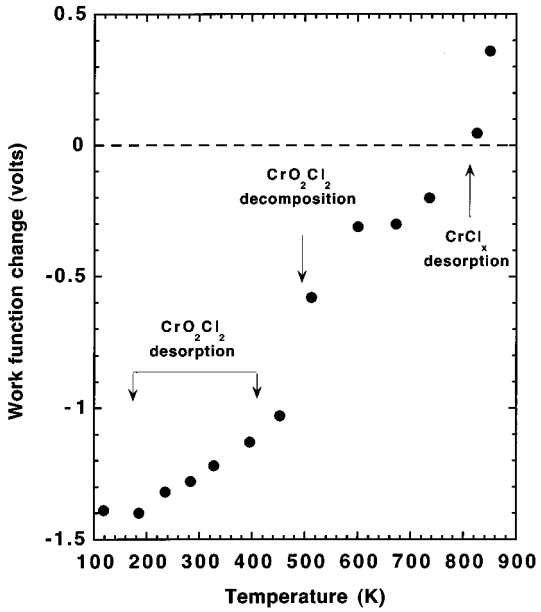

Figure 8. Work function change as a function of heating temperature for a CrO_2Cl_2 exposure of 1.3×10^{15} molecules/cm^2 on the clean TiO_2-(110) surface. Data were obtained after recooling.

distance is roughly 0.7 Å too small to accommodate Cl−Cl van der Waals repulsions. These repulsions are removed if the [001] rows of bidentate CrO_2Cl_2 are staggered instead of eclipsed.

The saturation CrO_2Cl_2 coverage measured by TPD is 0.65 ML (see Figure 3). For reasons discussed below, we assume that the 430 K CrO_2Cl_2 TPD peak, which constitutes about 0.09 ML of the adlayer, is due to desorption from defect sites. Subtracting this amount from the total yields a saturation coverage at nondefect sites of about 0.56 ML, or roughly three CrO_2Cl_2 molecules per every five surface Ti^{4+} sites. The coverage of a purely bidentate-bonded adlayer cannot, however, exceed 0.5 ML, so an additional species with a different bonding geometry must be present. An adlayer comprised of mostly bidentate CrO_2Cl_2 with some monodentate molecules (see Figure 7) could exceed a coverage of 0.5 ML. The TPD data suggest that roughly 0.48 ML of CrO_2Cl_2 decomposes and that 0.09 ML desorbs in the 295 K state. Given these constraints, a model for monolayer saturation of the nondefect sites at 130 K would be for two-thirds of the adlayer to be bidentate and one-third to be monodentate. Desorption of half of the monodentate molecules followed by conversion of the remaining monodentate species to bidentate species would give approximately half of a monolayer of bidentate CrO_2Cl_2 and a tenth of a monolayer of monodentate desorption. This is consistent with the TPD data. At 295 K we expect surface diffusion of bidentate species to be facile enough (based on the diffusion of bidentate formate on TiO_2(110)[28]) to allow the remaining monodentate molecules to find unoccupied sites and form new bidentate species.

The effect of annealing temperature on the work function change is shown in Figure 8. The $\Delta\Phi$ value for an adsorbed multilayer at 118 K is −1.4 V. Removal of multilayer CrO_2-Cl_2 (below 160 K) does not significantly change the work function. However, desorption of the monolayer between 160 and 450 K results in a +0.36 V change. At this temperature, we assume that the surface contains roughly 0.5 ML of bidentate CrO_2Cl_2. We can estimate the work function change (relative to the clean surface) resulting from the presence of this adlayer using the Helmholtz equation.[29] If we assume the adsorbed bidentate CrO_2Cl_2 has approximately the same dipole moment as that calculated by Pershina and Fricke for the gas-phase molecule,[25] then the estimated work function change is −0.86 V. This is close to the −1.03 V change (relative to the clean surface) measured after heating to 450 K (Figure 8). The difference between these two values may reflect the degree of charge transfer occurring between the adlayer and the surface or it may indicate that the 430 K TPD CrO_2Cl_2 TPD state had not been completely removed by heating to 450 K. Above 450 K, $\Delta\Phi$ increases rapidly and reaches −0.33 V at 600 K. This rise is associated with the decomposition of CrO_2Cl_2 (to be discussed later) and the retention of the electronegative decomposition products on the surface. Upon further heating, $\Delta\Phi$ continues to increase due to the desorption of $CrCl_x$ and reaches a value of +0.35 V at 850 K.

3.1.4. SSIMS Results. TPD data (discussed above) indicate that only about 26% of the CrO_2Cl_2 monolayer adsorbed on TiO_2(110) desorbs as molecular CrO_2Cl_2, while the remainder irreversibly decomposes on the surface. The decomposition products recombine to yield $CrCl_x$, which desorbs above 710 K. Since no oxygen-bearing decomposition products were detected by TPD, the fate of oxygen remains uncertain. Isothermal and temperature-programmed SSIMS measurements were carried out to address this uncertainty.

Positive SSIMS spectra from a clean TiO_2(110) surface and from a surface after CrO_2Cl_2 exposure of 1.9×10^{15} molecules/cm^2 at 130 K followed by TPD up to 820 K are presented in Figure 9. The naturally occurring isotopes of Ti range from 46 to 50 amu; however, only those Ti-containing ions associated with ^{48}Ti are labeled in Figure 9. The two spectra are scaled so that the $^{48}Ti^+$ ion peaks have the same intensity. Cr has naturally occurring isotopes at 50 and 52−54 amu, but only those Cr-containing ions associated with ^{52}Cr are labeled in Figure 9. Clearly, significant amounts of Cr remain on the surface after TPD up to 820 K as $CrCl_x$ (presumably), since the rate of $CrCl_x$ desorption peaks at 835 K. A weak CrO^+ (compared to Cr^+) +SSIMS ion signal suggests that a surface chromium oxide phase is not formed, although the MO^+/M^+ SIMS ratio is not a direct indicator of the M:O stoichiometry.[30] A weak +SSIMS ion signal from $TiCl^+$ suggests that some of the lattice oxygen has been replaced by chlorine. The presence of this ion mass is in agreement with the TPD data, which indicates a weak desorption signal for a $TiCl_x$ species. The −SSIMS spectrum from the clean TiO_2(110) surface showed only a weak O^- (m/e = 16) signal (spectra not shown). A

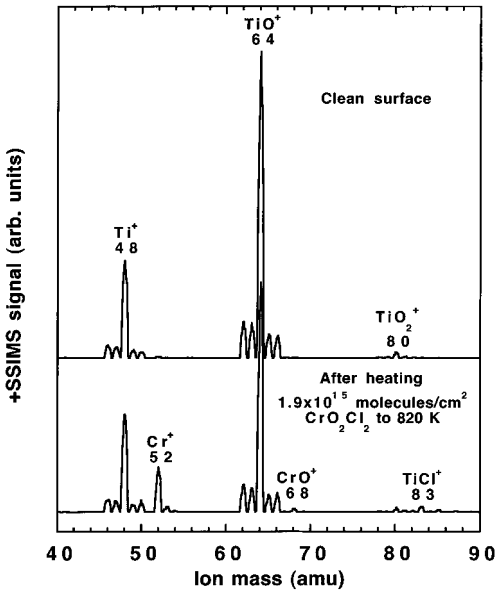

Figure 9. +SSIMS spectra from a clean TiO_2(110) surface and after heating a CrO_2Cl_2 exposure of 1.9×10^{15} molecules/cm^2 adsorbed at 130 to 820 K. The spectra are normalized to the $^{48}Ti^+$ peak intensities.

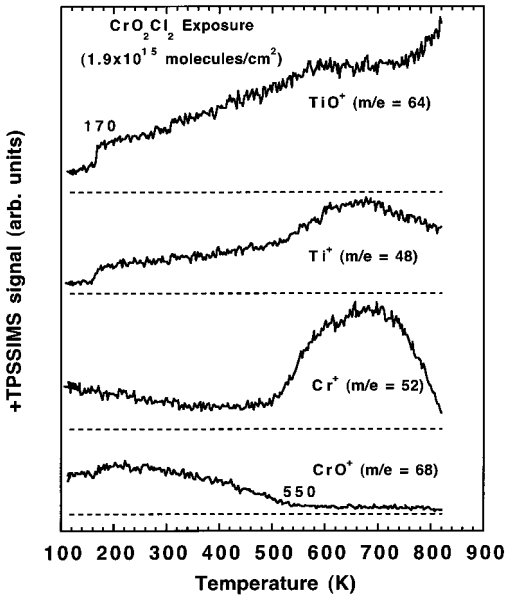

Figure 10. +TPSSIMS spectra from a CrO_2Cl_2 exposure of 1.9×10^{15} molecules/cm^2 to the clean TiO_2(110) surface at 130 K. Spectra are displaced vertically for clarity. Dashed lines indicate 0 counts/s levels for each ion.

−SSIMS spectrum from the clean TiO_2(110) surface exposed to CrO_2Cl_2 exposure of 2.0×10^{15} molecules/cm^2 at 130 K followed by TPD up to 820 K also showed a weak signal from O^-, along with weak signals from the naturally occurring isotopes of Cl (m/e = 35, 37). The −SSIMS ion signals from these two cases were weak because the work function of the surface (see Figures 6 and 8) favored positive ion emission. However, as will be shown below, significant −SSIMS signals were detected when the work function was decreased by CrO_2Cl_2 adsorption.

Temperature-programmed SSIMS (TPSSIMS) was also used to determine the temperature range in which CrO_2Cl_2 chemistry occurred on TiO_2(110). The +TPSSIMS results from the Ti^+, Cr^+, TiO^+, and CrO^+ ions during heating of a 1.9×10^{15} molecules/cm^2 exposure of CrO_2Cl_2 at 130 K on a clean TiO_2(110) surface are presented in Figure 10. Similar results were obtained at lower exposures. The Ti^+ and TiO^+ ion signals are low between 130 and 160 K because the surface is covered with a multilayer of CrO_2Cl_2. The rapid increase in the Ti^+ and TiO^+ signals between 160 and 180 K is due to desorption of the CrO_2Cl_2 multilayer (see Figure 2b). The gradual increase in the Ti^+ and TiO^+ signals between 180 and 480 K is due to desorption of the CrO_2Cl_2 monolayer that exposes more TiO_2 surface and also increases the work function (see Figure 8). The somewhat rapid increase in the Ti^+ signal between 480 and 680 K can be linked to the work function change but also indicates surface chemical changes, since no thermal desorption occurs in this temperature range. Above 660 K, the Ti^+ and TiO^+ signals no longer track each other with the TiO^+/Ti^+ ratio increasing, suggestive of a change in the surface O:Ti stoichiometry toward a more oxidized condition (discussed later). The change at high temperature may also be associated with the desorption of $CrCl_x$. The Cr^+ and CrO^+ ion signals are the dominant signals from multilayer CrO_2Cl_2. These ion signals do not change significantly as the multilayer desorbs but decrease as the surface is heated to 490 K. At this point the CrO^+ signal continues to decrease, but the Cr^+ signal increases between 490 and 680 K before falling to near zero at 820 K. The initial decrease in the Cr^+ and CrO^+ signals is due to the desorption and decomposition of monolayer CrO_2Cl_2. The increase in the Cr^+ signal between 490 and 680 K is due to the formation of a new surface species (presumably $CrCl_x$), and the subsequent decrease after 680 K is due to the desorption of $CrCl_x$.

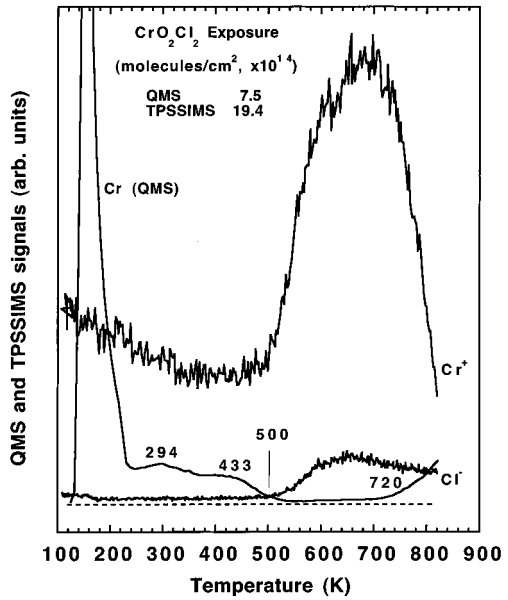

Figure 11. TPD spectrum of the Cr^+ (m/e = 52) QMS cracking fragment and TPSSIMS spectra of Cr^+ (m/e = 52) and Cl^- (m/e = 35) from multilayer exposures of CrO_2Cl_2 to clean TiO_2(110) surface at 130 K. Dashed line indicates 0 counts/s levels for the SSIMS ions.

The changes in the +TPSSIMS shown in Figure 10 are better understood by comparing the Cr^+ TPSSIMS signal with that of the Cl^- TPSSIMS signal and the Cr TPD signal, all for a multilayer exposure of CrO_2Cl_2 on a clean TiO_2(110) surface at 130 K (Figure 11). The Cl^- signal is the dominant ion signal in −TPSSIMS. The Cr^+ and Cl^- ion signals follow each other, indicating that they reflect the same surface species. Correlation of these data with the Cr TPD signal indicates that the TPSSIMS signals do not begin to increase until the Cr TPD signal drops to near the background level. However, the TPSSIMS signals decrease coincidentally with the increase in the Cr TPD signal above 720 K. These comparisons suggest that $CrCl_x$ formation

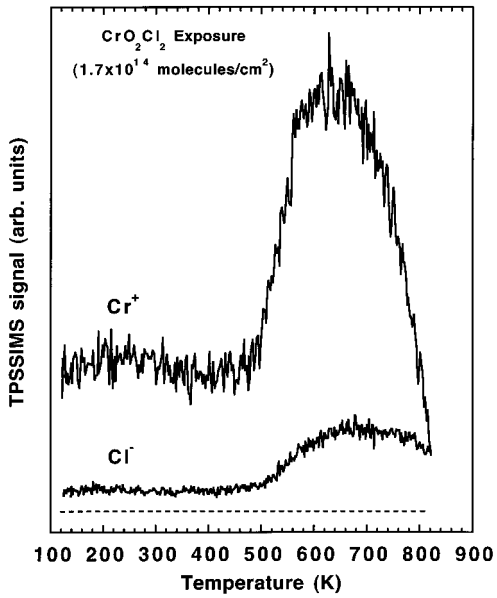

Figure 12. Cr^+ ($m/e = 52$) and Cl^- ($m/e = 35$) ion signals during +TPSSIMS and −TPSSIMS, respectively, from CrO_2Cl_2 exposure of 1.7×10^{14} molecules/cm^2 to clean TiO_2(110) surface at 130 K. Dashed line indicates 0 counts/s levels for each ion.

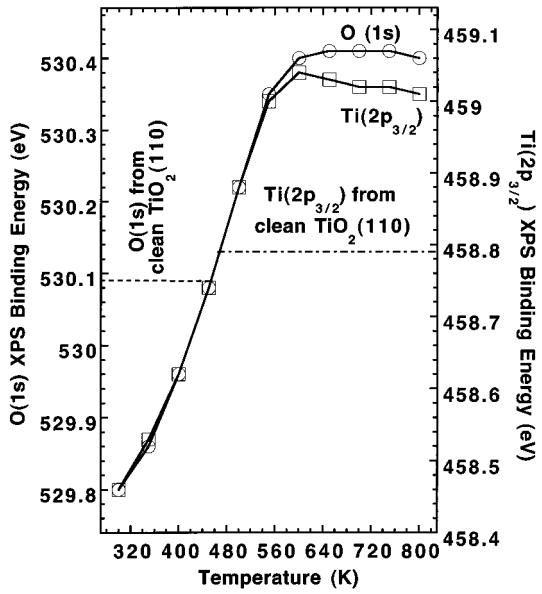

Figure 13. Changes in the Ti($2p_{3/2}$) (□) and O(1s) (○) XPS BEs as a result of heating a saturated monolayer of CrO_2Cl_2 adsorbed on TiO_2-(110) at 300 K. The left and right *y*-axes have the same range and were referenced to each other by the 300 K data. Dashed lines represent the respective clean surface BEs.

and CrO_2Cl_2 desorption are not directly correlated and that the Cr^+ and Cl^- TPSSIMS signals above 500 K result from $CrCl_x$ formation.

Further evidence for decomposition of CrO_2Cl_2 at temperatures above 500 K is obtained from the Cr^+ and Cl^- TPSSIMS signals from a 1.7×10^{14} molecules/cm^2 exposure on clean TiO_2(110) at 130 K (Figure 12). TPD from this exposure indicates that all adsorbed CrO_2Cl_2 decomposes without any CrO_2Cl_2 desorption. The Cr^+ and Cl^- TPSSIMS signals are constant between 130 and 500 K and increase above 500 K just as was observed for higher exposures (Figure 11). This strongly suggests that adsorbed CrO_2Cl_2 does not decompose on TiO_2(110) until temperatures above 500 K.

3.1.5. XPS Results. XPS experiments monitoring the Cr($2p_{3/2}$), the poorly resolved Cl($2p_{3/2,1/2}$) doublet (hereafter referred to as Cl(2p)), the Ti($2p_{3/2}$), and the O(1s) features were performed on a TiO_2(110) surface saturated with CrO_2Cl_2 at 300 K (see Experimental Section) and after being heated to various temperatures. TPD data for CrO_2Cl_2 adsorbed on TiO_2-(110) at 300 K (not shown) are consistent with what would be expected based on the data in Figure 2; that is, the parent desorption state at 430 K and the $CrCl_x$ state above 700 K are observed with approximately the same TPD peak area as seen in the 130 K dosing experiments.

The adsorption of CrO_2Cl_2 on clean TiO_2(110) at 300 K results in an upward bending of the valence and conduction bands, as inferred in Figure 13, by the nearly equivalent shifts in the Ti($2p_{3/2}$) and O(1s) XPS peaks toward lower BEs relative to their clean surface peak positions (dashed lines). It should be noted that the O(1s) feature from CrO_2Cl_2 was not distinguishable from the O(1s) feature for TiO_2(110). In fact, the O(1s) fwhm was about 1.84 eV regardless of whether the surface was clean or CrO_2Cl_2 covered. For convenience, the O(1s) (circles) and Ti($2p_{3/2}$) (squares) BEs at 300 K are overlayed to show the shifts in these peaks as the surface is heated. Note that both the right and left *y*-axes have the same total range. As the surface was heated above 300 K, the Ti($2p_{3/2}$) and O(1s) XPS peaks shift to higher BEs at the same rate, indicating that the bands are straightening. The flat band position is reached after heating to about 450−500 K. Although we assume here that the clean surface BEs for Ti($2p_{3/2}$) and O(1s) reflect a flat band situation, especially since the Ti($2p_{3/2}$) BE matches those recorded in the literature for TiO_2(110),[31,32] the clean surface condition may also have some band bending due to the presence of small amounts of defect sites (see Experimental Section). Coincidentally, the 450−500 K range for reaching a flat band is the same temperature regime in which all parent CrO_2Cl_2 desorption is complete (see Figure 2) but prior to decomposition of the remaining adsorbed CrO_2Cl_2 (see Figures 11 and 12). At this point TPD estimates that the surface contains roughly 0.48 ML (2.5×10^{14} molecules/cm^2) of CrO_2Cl_2, or one CrO_2Cl_2 per every two surface Ti^{4+} sites. As decomposition of the CrO_2-Cl_2 adlayer begins (above 500 K), the bands bend downward and reach a constant downward bending after heating to about 600 K. This temperature corresponds roughly to the point at which all the adsorbed CrO_2Cl_2 has decomposed (see Figures 8, 11, and 12) but prior to the point at which any $CrCl_x$ is observed in TPD. Above 600 K the bands appear to remain relatively unchanged despite the fact that $CrCl_x$ desorption is taking place.

Before continuing with the discussion of the changes in the Cr($2p_{3/2}$) and Cl(2p) XPS features, we should address the source of the upward band bending due to CrO_2Cl_2 adsorption and its implications on photochemistry. The trends in the Ti($2p_{3/2}$) and O(1s) BEs during heating of the CrO_2Cl_2 adlayer suggest that the bands are bent not because of the presence of CrO_2Cl_2 per se but because of the CrO_2Cl_2 molecules that molecularly desorb in the 430 K TPD state. Based on TPD, this coverage is only about 9% of the fully saturated monolayer, or roughly 4×10^{13} molecules/cm^2. Since we know that this is about the level of oxygen vacancies on our surface (see Experimental Section), we suspect that the bands are bent as a result of charge transfer from these defect sites into CrO_2Cl_2 molecules adsorbed at these sites. Such a transfer of charge from the surface into the adlayer would result in a net positive charge in the near-surface region and cause the bands to bend upward. The consequence of this would be that photooxidation would be favored at the surface while photoexcited conduction electrons would move into the bulk of the oxide. This, of course, would not be favorable for

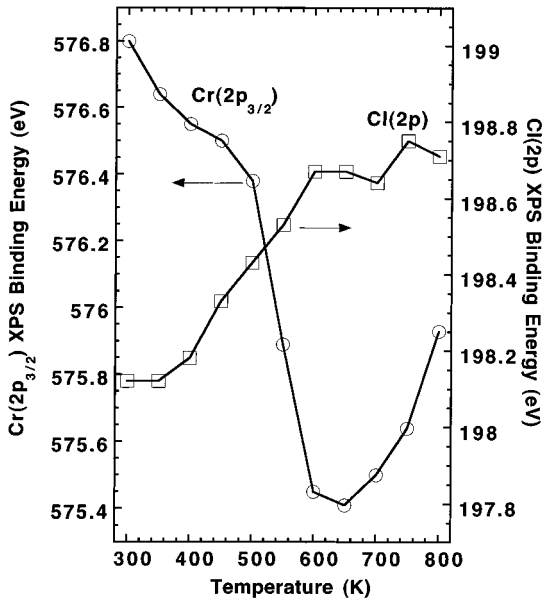

Figure 14. Changes in the $Cr(2p_{3/2})$ (○) and Cl(2p) (□) XPS BEs as a result of heating a saturated monolayer of CrO_2Cl_2 adsorbed on TiO_2-(110) at 300 K. The effects of band bending (see Figure 13) have been removed from the data.

the photoreduction of Cr(VI) to Cr(III). However, this case appears to be restricted to a surface in which isolated Ti^{3+} cations at oxygen vacancies sites are present, since the bands appear to flatten after CrO_2Cl_2 is desorbed from these sites. It is interesting to note that if the 430 K parent TPD state is associated with isolated Ti^{3+} cation sites, then these reduced cations do not bind a strong Lewis base, such as CrO_2Cl_2, as well as do the Ti^{4+} sites, which in this case dominate the TiO_2(110) surface and participate in CrO_2Cl_2 decomposition. This conclusion is consistent with previous findings for the binding of a weaker Lewis base, water, to TiO_2.[20, 22]

To show how the $Cr(2p_{3/2})$ and Cl(2p) XPS features change due to CrO_2Cl_2 chemistry on TiO_2(110), the effects of band bending were removed from the data. Figure 14 shows the BE changes for the $Cr(2p_{3/2})$ and Cl(2p) XPS peak positions after correcting for band bending for the TiO_2(110) surface saturated with CrO_2Cl_2 at 300 K and after heating this surface to various temperatures. At 300 K, the $Cr(2p_{3/2})$ XPS peak position for adsorbed CrO_2Cl_2 is at about 576.8 eV, with the position shifting by 0.4 eV to lower BEs as the remaining parent is desorbed between 300 and 500 K. The $Cr(2p_{3/2})$ peak also sharpens with heating, from a fwhm of 3.3 eV at 300 K to 2.3 eV after heating to 500 K. The sharpening of the $Cr(2p_{3/2})$ peak is consistent with the model suggested above for CrO_2Cl_2 desorption from defect sites. However, the $Cr(2p_{3/2})$ peak shifts by about 1.0 eV and broadens to a fwhm of about 3.9 eV as the surface is heated above 500 K to about 600 K. Although it is often difficult to assign an oxidation state due the $Cr(2p_{3/2})$ peak position, this shift suggests a significant change in the chemical state of the Cr atom such as that of a reduction process. This change in the $Cr(2p_{3/2})$ peak position is coincident with changes in the Cr^+ and Cl^- temperature-programmed SSIMS signals (Figures 10 and 11) and a +0.7 V $\Delta\Phi$ (Figure 8) between 500 and 600 K. After reaching 650 K, most of the adsorbed CrO_2-Cl_2 has decomposed, as inferred from the SSIMS data, and the $Cr(2p_{3/2})$ peak position has reached a minimum at about 575.4 eV. As the temperature is increased above 700 K and $CrCl_x$ is desorbed, the $Cr(2p_{3/2})$ peak shifts to higher BE. After being heated to 800 K, the Cr remaining on the surface has a $Cr(2p_{3/2})$ XPS BE of about 575.9 eV, which is consistent with Cr in the 3+ or 4+ oxidation state.[33] Also, Pan and co-workers[34] observed a $Cr(2p_{3/2})$ XPS BE of about 575.8 eV for a Cr suboxide phase on TiO_2(110). Scharf et al.[35] noted $Cr(2p_{3/2})$ XPS BEs in the 575−577 eV range from CrO_x films supported on TiO_2 (Degussa P-25) after $Cr(NO_3)_3$ impregnation and calcination.

The reduction of the Cr species resulting from CrO_2Cl_2 decomposition could be the result of one or more possibilities. For example, the TiO_2 crystal, which is n-doped as a result of vacuum annealing, could act as the reducing agent. This would involve more than the charge in the estimated $(2.5-5) \times 10^{13}$/cm^2 of oxygen vacancies sites in the surface, since reduction of the Cr^{6+} in roughly 0.5 ML of CrO_2Cl_2 would require an order of magnitude more Ti^{3+} cations. Interstitial Ti^{3+} cations are believed to be the dominate bulk electron defects in nominally vacuum-reduced TiO_2.[36] These reduced cations may diffuse from the bulk to the surface and be oxidized. This would also explain why, based on TPD, all of the oxygen from CrO_2-Cl_2 decomposition remains on the surface. However, the rate of thermal diffusion of these charge carriers may be slow below 650 K based on temperature-programmed SSIMS studies.[37] It may also be possible that the reduction of Cr^{6+} in the decomposed parent results from electrons conducted from ground. In this case the destination of the deposited oxygen remains a mystery, especially since the stoichiometry of the $CrCl_x$ desorption product appears to be the same as in the parent molecule (see below).

The Cl(2p) XPS peak behaves in a manner opposite from that of the $Cr(2p_{3/2})$ peak. As the heating temperature is raised from about 350 to 600 K, the Cl(2p) XPS peak shifts from about 198.1 to 198.7 eV with approximately half of the shift occurring between 450 and 600 K. Above 600 K the Cl(2p) peak position remains relatively constant, although the area of the peak steadily decreases due to $CrCl_x$ desorption.

3.2. Results from the ^{18}O-Enriched Surface. It was mentioned earlier that CrO_2Cl_2 desorption is a fraction (∼26%) of the amount adsorbed and no oxygen-bearing decomposition products were detected by TPD. The fate of oxygen, therefore, remains a mystery. To address this issue, decomposition of CrO_2Cl_2 adsorbed on a clean ^{18}O-enriched TiO_2(110) surface (see Experimental Section) was studied by TPD and SSIMS.

Figure 15 shows TPD spectra for the $^{52}Cr^{16}O$ (m/e = 68) and $^{52}Cr^{18}O$ (m/e = 70) QMS signals from TPD of the clean, ^{18}O-enriched TiO_2(110) surface exposed at 130 K to 4.1×10^{14} molecules/cm^2 of CrO_2Cl_2. The signals for these isotopes were deconvoluted from that of other species appearing at the same m/e values (for example, $^{54}Cr^{16}O$) using the naturally occurring abundances and matrix algebra. The TPD trace of $^{52}Cr^{16}O$ (m/e = 68) is identical with that of the parent molecule $^{52}Cr^{16}O_2Cl_2$ (m/e = 154, not shown) except in intensity, suggesting that the two traces have the same origin, consistent with the earlier conclusion that $^{52}Cr^{16}O$ does not desorb from the surface. Comparison of the $^{52}Cr^{16}O$ and $^{52}Cr^{18}O$ signals suggests that the parent desorption in the 430 K TPD state has undergone exchange with the lattice. This exchange could be either the result of a molecular process that does not involve a stable intermediate or the result of dissociative recombination involving a stable $CrOCl_2$ surface intermediate. On the basis of the approximately equivalent amounts of parent in the 295 and 430 K TPD states and on the total amount of parent desorption, we estimate that no more than about 13% of the adsorbed CrO_2Cl_2 monolayer (4.4×10^{13} molecules/cm^2) exchanges oxygen with the lattice. This amount of exchange would involve an approximately equivalent number of surface sites, further

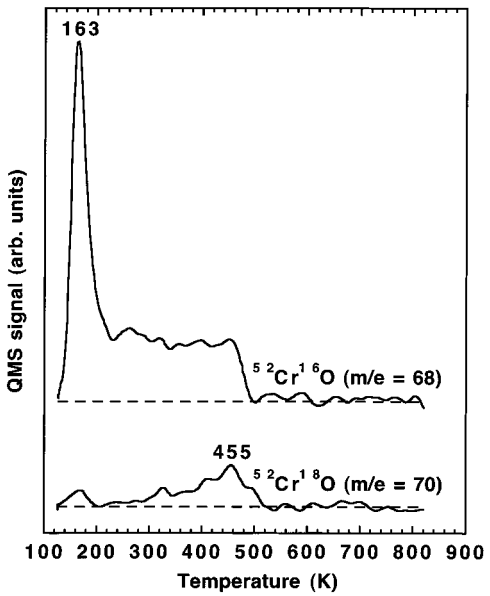

Figure 15. TPD spectra from a CrO_2Cl_2 exposure of 4.1×10^{14} molecules/cm^2 to the clean ^{18}O-enriched $TiO_2(110)$ surface at 130 K. Spectra are displaced vertically, and baselines are shown to highlight the important TPD features.

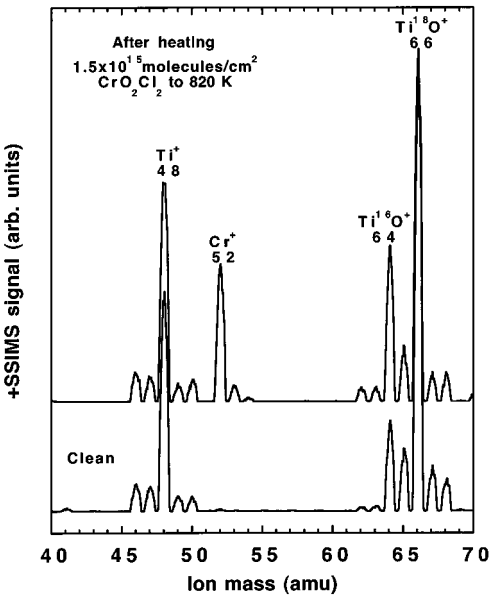

Figure 16. +SSIMS spectra from a clean ^{18}O-enriched $TiO_2(110)$ surface and after heating a CrO_2Cl_2 exposure of 1.5×10^{15} molecules/cm^2 adsorbed at 130 to 820 K. The spectra are normalized to the $^{48}Ti^+$ peak intensities.

suggesting that oxygen vacancy sites are associated with the 430 K parent TPD state.

The TPD data discussed above indicates that limited exchange of oxygen occurs between the lattice and the parent molecule. This observation does not shed light on the fate of the oxygen from CrO_2Cl_2 decomposition. To further address this issue, positive SSIMS spectra are presented in Figure 16 from a clean ^{18}O-enriched $TiO_2(110)$ surface and from a ^{18}O-enriched surface after CrO_2Cl_2 exposure of 1.5×10^{15} molecules/cm^2 at 130 K followed by heating to 820 K. The two spectra are scaled so that the $^{48}Ti^+$ ion peaks have the same intensity. After deconvolution of contributing isotopic signals, the $Ti^{18}O^+/Ti^{16}O^+$ intensity ratio for the clean sample is about 11.2, indicating that not all ^{16}O in the SSIMS probing depth was replaced by oxidation with $^{18}O_2$. This ratio, however decreases

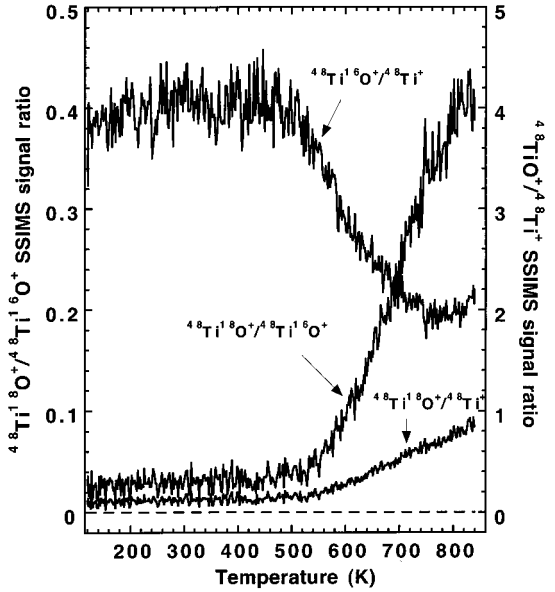

Figure 17. +TPSSIMS during exposure of 5.0×10^{-7} Torr of $^{18}O_2$ to clean $Ti^{16}O_2(110)$. The ion signal ratios were determined after deconvolving contributions from other Ti isotopes. Residual $^{48}Ti^{18}O^+$ in the low-temperature region (<500 K) resulted from trace ^{18}O that remained in the surface from a previous experiment.

to 2.8 after the CrO_2Cl_2 exposed surface is heated to 820 K. This large change in the ^{18}O:^{16}O ratio cannot be explained by the small amount of oxygen exchange between the lattice and the parent molecule observed by TPD. Instead, the ^{16}O brought by the parent is being incorporated into the surface. Also, a significant amount of Cr remains on the surface after heating to 820 K, presumably as $CrCl_x$.

The ability of the oxidized surface to accommodate additional oxygen from CrO_2Cl_2 decomposition is discussed above but can also be better understood by examining Figure 17. In this experiment the fully oxidized $TiO_2(110)$ surface is exposed at 120 K to an $^{18}O_2$ backfill pressure of 5.0×10^{-7} Torr (a flux of 1.7×10^{14} molecules cm^{-2} s^{-1}), and the crystal temperature is ramped to 840 K while various SSIMS signals were monitored. After the deconvolution of contributions from other isotopes as described above, the $^{48}Ti^{16}O^+$ and the $^{48}Ti^{18}O^+$ SSIMS signals are expressed in terms of the $^{48}Ti^{18}O^+/^{48}Ti^{16}O^+$, $^{48}Ti^{18}O^+/^{48}Ti^+$, and $^{48}Ti^{16}O^+/^{48}Ti^+$ ion ratios. Note that both the $^{48}Ti^{16}O^+/^{48}Ti^+$ and $^{48}Ti^{18}O^+/^{48}Ti^+$ ratios are constant between 120 and 520 K, with the former near a value of 4, consistent with an oxidized surface, and the latter near zero (some residual ^{18}O remained in the sample from previous experiment). However, as the surface temperature exceeds 520 K, the $^{48}Ti^{16}O^+/^{48}Ti^+$ ratio decreases and the $^{48}Ti^{18}O^+/^{48}Ti^+$ ratio increases, reflective of isotopic exchange occurring between gas-phase $^{18}O_2$ and the $Ti^{16}O_2(110)$ surface. The $^{48}Ti^{18}O^+/^{48}Ti^{16}O^+$ ratio reveals that the rate of this exchange process is constant or increases as the temperature is raised from 520 to about 780 K.

The most logical explanation for the data in Figure 17 is not to view this process as $^{16}O-^{18}O$ exchange but as ^{18}O incorporation. By this we mean that oxygen vacancy sites are formed at temperatures above 520 K presumably by the desorption of $^{16}O_2$ from the surface although no oxygen signal ($m/e = 16$ or 32) was detected in TPD. Then because the bulk of the crystal is heavily reduced, these vacancy sites remain at the surface and are active for $^{18}O_2$ adsorption and dissociation. Of course, the overall kinetics for this process are probably much more complex than this because O_2 dissociation requires adjacent

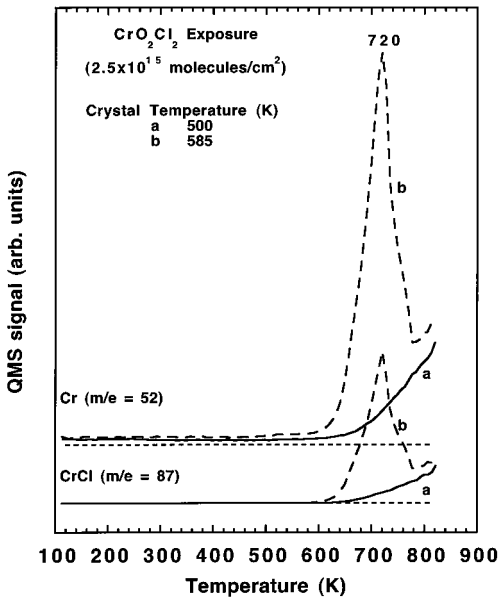

Figure 18. TPD spectra from a 2.5×10^{15} molecules/cm^2 CrO_2Cl_2 exposure to the clean TiO_2(110) surface as a function of crystal temperature. Spectra are displaced vertically for clarity.

vacancy sites (which is why approximately 0.05−0.10 ML of isolated vacancy sites remain on the surface after oxidation treatment) and because there are probably strong temperature dependencies in the surface and surface−bulk diffusion. Nevertheless, these data suggest that the creation of surface vacancies sites may play a role in the decomposition of adsorbed CrO_2Cl_2 and may also explain why no oxygen-containing decomposition products are observed in TPD.

3.3. Effect of Adsorption Temperature. To further understand the significant changes in the SSIMS, XPS, and $\Delta\Phi$ data occurring between 500 and 650 K, we have conducted TPD, AES, and XPS experiments in which the crystal temperature was held below and above this temperature regime during CrO_2Cl_2 dosing.

Figure 18 shows Cr (m/e = 52) and CrCl (m/e = 87) TPD spectra obtained after CrO_2Cl_2 exposures of 2.5×10^{15} molecules/cm^2 to the clean TiO_2(110) surface at 500 and 585 K. The spectra were taken after recooling to 130 K. As expected, neither multilayer nor monolayer desorption peaks are observed at dosing temperatures of 500 and 585 K because both these states desorb below 500 K. At a dosing temperature of 500 K, the CrCl signal appears at 650 K and continues to rise in intensity up to 820 K. This feature is essentially identical with that observed in spectra where the crystal temperature was 130 K (see Figures 1 and 2). Upon CrO_2Cl_2 exposure at a crystal temperature of 585 K, the CrCl signal exhibits a sharp desorption peak at 720 K. Comparison of TPD spectra taken from various CrO_2Cl_2 exposures dosed at 585 K (data not shown) reveals that the 720 K $CrCl_x$ TPD state exhibits zeroth-order desorption kinetics (leading edges overlay and the peak temperature shifts higher with increasing exposure). Zeroth-order rate analysis for this $CrCl_x$ TPD state yields an activation energy of desorption of 206 ± 3 kJ/mol. This value is close to the 210 ± 15 kJ/mol barrier determined by Foord and Lambert[38] for the desorption of a thick $CrCl_x$ film grown on Cr(100) by reaction with Cl_2. QMS signals during desorption of the $CrCl_x$ film on Cr(100) were detected at m/e values corresponding to Cl, Cr, CrCl, and $CrCl_2$ species, but no signal was detected at m/e values corresponding to $CrCl_3$ or higher chlorides. Additionally, prior to desorption of the $CrCl_x$ film, Foord and Lambert observed a 575.8 eV Cr($2p_{3/2}$) feature, which they ascribed to Cr^{2+} in the film. These findings led the authors to conclude that the film was $CrCl_2$. The similarities between the TPD and XPS data of Foord and Lambert to those in this study are significant. Although the heats of sublimation of $CrCl_2$ and $CrCl_3$ are similar,[39] the absence of a desorption signal corresponding to $CrCl_3$ suggests the film is $CrCl_2$ or that the film decomposes to yield $CrCl_2$ during heating. Our XPS results (not shown) from CrO_2Cl_2 dosed at 625 K on TiO_2(110) give a single Cr($2p_{3/2}$) feature at about 576.6 eV (fwhm of 2.8 eV), suggestive of either Cr^{2+} or Cr^{3+}. However, as opposed to the case of Cl_2 on Cr(100), CrO_2Cl_2 adsorption at 585−625 K left a film that was composed of Cr, Cl, and O with significantly attenuated Ti signals, as indicated by AES and XPS. No oxygen-containing species was detected in TPD during decomposition of this film. The similarities to the work of Foord and Lambert suggest that the $CrCl_x$ signal above 700 K in the TPD of CrO_2Cl_2 is due to $CrCl_2$ desorption.

SSIMS (Figures 11 and 12) and XPS (Figure 14) results suggest that CrO_2Cl_2 adsorbed on TiO_2(110) at 130 K does not decompose until above 500 K. Therefore, it appears that the significant difference in TPD between dosing at a crystal temperature below 500 and above 550 K lies in the rate of CrO_2Cl_2 decomposition. Below 500 K the kinetics for CrO_2Cl_2 decomposition are slow and the monolayer becomes saturated during dosing with CrO_2Cl_2 and/or one of its decomposition intermediates. This is consistent with the findings of Drozd et al.,[40] who used CrO_2Cl_2 adsorption in the 375−475 K temperature range to grow ALE (atomic layer epitaxy) films of chromium oxide−aluminum oxide on Si. These authors noted that the deposited chromium oxide layer was more than a monolayer thick when the adsorption temperature exceeded 500 K. Similarly, above 550 K the kinetics for CrO_2Cl_2 decomposition on TiO_2(110) are fast, and the surface is not passivated but continues to decompose CrO_2Cl_2 more or less independently of whatever species are being built up on the surface. This implies that one or more of the Cr−O and/or Cr−Cl bonds must break in this temperature regime. Unfortunately, we do not have any direct spectroscopic evidence supporting a mechanism for this decomposition process. However, it seems logical, based on our proposed bonding geometry for CrO_2Cl_2 and on the TPD products seen above 700 K, to propose that at least one of the Cr−O bonds is broken as the temperature exceeds 500 K. This assumption is supported by the estimation that the bond dissociation energy for the Cr−O bonds in gas-phase CrO_2Cl_2 is approximately 100 kJ/mol lower than that of the Cr−Cl bonds.[39]

4. Conclusions

The surface chemistry of CrO_2Cl_2 on TiO_2(110) is rich and complicated. We have shown that this molecule binds very strongly to the surface and is stable up to 500 K. The monolayer saturation coverage appears to be 0.65 ML (1 ML = 5.2×10^{14} sites/cm^2), although about 0.09 ML is more weakly held at isolated oxygen vacancy sites and desorbs molecularly at 430 K. An additional 0.09 ML desorbs at 295 K, leaving about 0.48 ML to irreversibly decompose above 500 K. The decomposed layer then evolves $CrCl_2$ in TPD above 700 K with all of the deposited oxygen presumably remaining on the surface. The thermal reduction of Cr(VI) in CrO_2Cl_2 to a species that evolves Cr(II) as $CrCl_2$ probably results from oxidation of the n-doped TiO_2(110) crystal.

Acknowledgment. This work was supported by the U.S. DOE, Office of Basic Energy Sciences, Division of Materials

Science and by the U.S. DOE Environmental Management Science Program. M. Alam is indebted to the Associated Western Universities, Inc. for providing a summer fellowship and for supporting this research under Grants DE-FG06-92RL-12451, DE-FG07-93ER-75912, and DE-FG07-94ID-13228 with the U.S. Department of Energy. P.D.K. thanks the Associated Western Universities, Inc., Northwest Division for a postdoctoral fellowship. AWU-NW is supported by Grant DE-FG06-89ER-75522 with the U.S. DOE. We also thank Scott Chambers and John Daschbach for helpful discussions on the topic of band bending.

References and Notes

(1) Patterson, J. W. *Industrial Waste Water Treatment Technology*, 2nd ed.; Butterworth: Stoneham, 1985; p 53.
(2) Kapil, V. *Chromium Toxicity*; U.S. Department of Health and Human Services, Public Health Services, Agency for Toxic Substances and Disease Registry: Atlanta, 1990; pp 2−3, 16−17.
(3) Gross, D. W. *J. Air Pollut. Control Assoc*. **1986**, *36*, 603.
(4) Yoneyama, H.; Yamashita, Y.; Tamura, H. *Nature* **1979**, *282*, 817.
(5) Munoz, J.; Domenech, X. *J. Appl. Electrochem*. **1990**, *20*, 518.
(6) Xu, Y.; Chen, X. *Chem. Ind.* **1990**, *15*, 497.
(7) Sabate, J.; Anderson, M. A.; Aguado, M. A.; Giminez, J.; Cervera-March, S.; Hill, Jr. C. G. *J. Mol. Catal.* **1992**, *71*, 57.
(8) Lin, W.; Wei, C.; Rajeshwar, K. *J. Electrochem. Soc*. **1993**, *140*, 2477.
(9) Prairie, M. R.; Evans, L. R.; Stange, B. M.; Martinez, S. L. *Environ. Sci. Technol*. **1993**, *27*, 1776.
(10) Zachara, J. M.; Girvin, D. C.; Schmidt, R. L.; Resch, C. T. *Environ. Sci. Technol.* **1987**, *21*, 589.
(11) Davis, J. A.; Leckie, J. O. *J. Colloid Interface Sci*. **1980**, *74*, 33.
(12) Wehrli, B.; Ibric, S.; Stumm, W. *Colloids Surf.* **1990**, *51*, 77.
(13) Alam, M.; Henderson, M. A. In preparation.
(14) Udy, M. J. *Chromium: Chemistry of Chromium and its Compounds*; Reinhold: New York, 1956; p 192.
(15) Jacobson, C. A. *Encyclopedia of Chemical Reactions*; Reinhold: New York, 1948; p 764.
(16) Mehandjiev, D.; Angelov, S.; Damyanov, D. *Stud. Surf. Sci. Catal*. **1979**, *3*, 605.
(17) McDaniel, M. P. *J. Catal*. **1982**, *76*, 17.
(18) Damyanov, D.; Vlaev, L. *Bull. Chem. Soc. Jpn*. **1983**, *56*, 1841.
(19) Nishimura, M.; Thomas, J. M. *Catal. Lett*. **1993**, *21*, 149.
(20) Henderson, M. A. *Surf. Sci*. **1994**, *319*, 315.
(21) Henderson, M. A. *Surf. Sci.* **1996**, *355*, 151.
(22) Henderson, M. A. *Langmuir* **1996**, *12*, 5093.
(23) Linsebigler, A. Private communications. Lu, G.; Linsebigler, A.; Yates, J. T., Jr. *J. Phys. Chem*. **1994**, *98*, 11733.
(24) Masel, R. I. *Principles of Adsorption and Reaction on Solid Surfaces*; Wiley-Interscience: New York, 1996; p 513.
(25) Pershina, V.; Fricke, B. *J. Phys. Chem*. **1996**, *100*, 8748.
(26) Chambers, S. A.; Thevuthasan, S.; Kim, Y. J.; Herman, G. S.; Wang, Z.; Tober, E.; Ynzunza, R.; Morais, J.; Peden, C. H. F.; Ferris, K.; Fadley, C. S. *Chem. Phys. Lett*. **1997**, *267*, 51.
(27) Marsden, C. J.; Hedberg, L.; Hedberg, K. *Inorg. Chem.* **1982**, *21*, 1115.
(28) Onishi, H.; Fukui, K.; Iwasawa, Y. *Colloids Surf. A* **1996**, *109*, 335.
(29) Besocke, K.; Krahl-Urban, B.; Wagner, H. *Surf. Sci.* **1977**, *68*, 39.
(30) Okajima, Y. *J. Appl. Phys.* **1984**, *55*, 230.
(31) Gopel, W.; Anderson, J. A.; Frankel, D.; Jaehnig, M.; Phillips, K.; Schafer, J. A.; Rocker, G. *Surf. Sci.* **1984**, *139*, 333.
(32) Gao, Y.; Liang, Y.; Chambers, S. A. *Surf. Sci.* **1996**, *348*, 17.
(33) Hanafi, Z. M.; Ismail, F. M.; Mohamed, A. K. *Z. Phys. Chem*. **1996**, *194*, 61.
(34) Pan, J. M.; Diebold, U.; Zhang, L.; Madey, T. E. *Surf. Sci.* **1993**, *295*, 411.
(35) Scharf, U.; Schneider, H.; Baiker, A.; Wokawn, A. *J. Catal*. **1994**, *145*, 464.
(36) Aono, M.; Hasiguti, R. R. *Phys. Rev. B* **1993**, *48*, 12406.
(37) Henderson, M. A. *Surf. Sci.* **1995**, *343*, L1156.
(38) Foord, J. S.; Lambert, R. M. *Surf. Sci*. **1982**, *115*, 141.
(39) Ebbinghaus, B. B. *Combust. Flame* **1995**, *101*, 311.
(40) Drozd, V. E.; Tulub, A. A.; Aleskovski, V. B.; Korol'Kov, D. V. *Appl. Surf. Sci.* **1994**, *82/83*, 587.